

UDC 621.314

## ANALYSIS OF TWO-SECTION PHASE-CONTROLLED RESONANT VOLTAGE CONVERTER

Anatolii Lupenko; Leonid Movchan; Ivan Sysak

*Ternopil Ivan Puluj National Technical University, Ternopil, Ukraine*

**Summary.** Analysis of two-section resonant DC-to-DC converter with phase power control is carried out in this paper. Two-section converter is considered as a boundary case of the multi-section converter with only one controlled section and other uncontrolled sections. The converter sections are parallel resonant half-bridge voltage inverters with a common resonant capacitor connected to the load through a matching transformer, center-tapped rectifier and smoothing filter. One of the sections is the reference, relative to which the phase shift of the output pulses of the other section is adjusted. The switching frequency of the converter is constant, which improves its electromagnetic compatibility. Analysis is carried out by the fundamental harmonic approximation method. Analytical expressions for voltage and current phasors in both sections of the converters have been established. The dependence of the converter power on the phase shift between the pulses of the half-bridge inverter sections was obtained. The dependence of the efficiency of the converter on the power was analyzed. It is shown that the efficiency slightly decreases when the power is reduced in a wide range of powers and only at powers less than 10% of full load power it drops sharply. The problems of operation of section transistor switches in their zero-voltage switching mode is considered. Verification of the conducted analysis was carried out by simulation of the converter circuit using the PSIM program for modeling power electronics devices. The simulation results are in a good agreement with the analysis results.

**Key words:** two-section resonant inverter, zero-voltage switching power, phase control, power, efficiency.

[https://doi.org/10.33108/visnyk\\_tntu2023.02.087](https://doi.org/10.33108/visnyk_tntu2023.02.087)

Received 02.03.2023

**Statement of the problem.** Resonant DC-DC converters (DCRC), which have been used in power electronics for about four decades and have gained significant popularity in recent years, are a class of switch converters of electrical energy parameters, one of the main parts of which is a resonant tank, which takes part in the energy processing and determines the properties of such converters [1–4]. DCRCs are used in such applications as chargers [5, 6], wireless energy transmission systems [7, 8], power sources of radio-electronic equipment [9, 10], drivers of LED light sources [11, 12]. In general, DCRC consists of a switch network (an inverter that converts the input DC voltage into rectangular pulses), resonant tank and a rectifier with a filter. To ensure galvanic isolation and the necessary voltage transfer ratio between the resonant tank and the rectifier, a transformer is placed. The main advantage of such DCRCs over PWM converters is their ability to provide «soft» switching of power transistors at zero voltage or at their zero current at the switching time interval [13, 14]. Therefore, the switching losses are significantly reduced, which makes it possible to increase the efficiency of converter. On the other hand, it allows to significantly increase the operating frequency, and therefore to reduce the value of the reactive components of the resonant tank and the rectifier filter. As a result, DCRCs have significantly better mass-volume parameter, i.e., higher power density compared to PWM converters. Along with this, the smoothness of the sine wave shape, due to the filtering property of the resonant tank, unlike the pulses of PWM converters, improves the electromagnetic compatibility of the DCRC.

**Analysis of the available investigation results.** A significant part of DCRC research is devoted to easy-to-implement resonant converters – series (SRC) [15, 16], parallel (PRC) [17, 18], series-parallel (SPRC) [19, 20]. In the role of a switching network, a highly efficient and compact half-bridge inverter [2, 18] is most often used, or bridge inverter [21]. In order to obtain higher output power, a multi-section structure of DCRCs are used, which consists of separate half-bridge resonant sections that work on a common load [22, 23]. In such a structure, the most expedient is the use of half-bridge SPRCs, since the addition of the power of each of the sections in the common load occurs in the mode of current sources, the role of which is performed by resonant inductances  $L$  (Fig. 1). At the same time, there is no need for auxiliary means of balancing the currents (powers) of individual sections.

Control of the output power of DCRC is mainly carried out by changing its switching frequency. At the same time, the switching frequency varies widely, which causes the disadvantages of such power control and requires additional efforts to maintain electromagnetic compatibility, to solve the problems of filtering, utilizing of power switches and magnetic components. Using the multi-section structure of DCRC, it is possible to eliminate these drawbacks by changing the phase shifts between the output pulses of individual half-bridge resonant sections when they operate at a constant frequency. Therefore, the study of such multi-section structures is of interest to scientists in the field of power electronics.

In this work, a two-section resonant DC-DC converter with phase power control is analyzed, considering it as a boundary case of a multi-section resonant inverter. A similar two-section converter is considered in [24], but in its analysis it is assumed that the phase shifts of the voltages of the resonant sections are mutually opposite and the same in magnitude, which goes beyond the concept of power control of multi-section DCRC and complicates the application of such an analysis for multi-section converters, where the phase shifts in inverter sections can be arbitrary (not the same) and independent of each other. In a multi-section converter, only one section can be taken as a reference (uncontrolled), relative to which the phase shifts of other (controlled) sections are adjusted. Then, by turning off the «redundant» sections, it is possible to provide less output power with a correspondingly smaller number of sections, which makes it possible to increase the efficiency of the multi-section converter at medium and low powers [23].

For the analysis of a two-section resonant DC-DC converter as a boundary case of a multi-section converter with phase control, this approach is proposed, in order to further develop it for the analysis of multi-section on-load tap-changers with an arbitrary number of sections.

**The objective of the paper** is to investigate the parameters and characteristics of two-section resonant DC-DC converter as a partial (simplest) case of a multi-section converter with phase power control while ensuring its constant operating frequency.

**Setting objectives.** The diagram of a two-section resonant converter is shown in Fig. 1. Each of its sections is a series-parallel resonant inverter, which consists of a half-bridge inverter on transistors  $M1, M2$  ( $M3, M4$ ), the outputs of which are connected to a common resonant capacitor  $C$  through a coupling capacitors  $C_s$  and an inductances  $L$ . An almost sinusoidal alternating voltage of the capacitor  $C$  is applied to the primary winding of the transformer  $T$ . Voltage of secondary winding is rectified by diodes  $D1, D2$ , and then through a smoothing filter  $L_f C_f$  is applied to the load  $R$ . A transformer with a turn ratio of  $n:1:1$  matches the loaded rectifier with inverter part and provides galvanic isolation of converter.

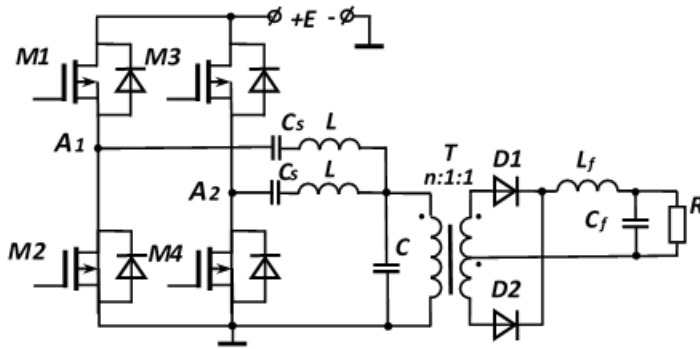


Figure 1. Two-section resonant converter

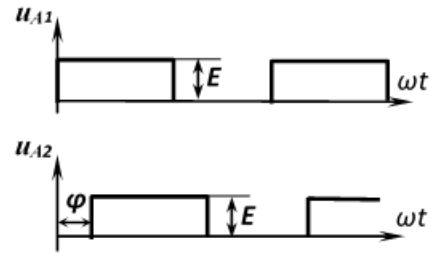


Figure 2. Half-bridge pulses

The voltages at the midpoints of half-bridges  $A1$  and  $A2$  are periodic rectangular pulses  $u_{A1}$  and  $u_{A2}$  respectively (Fig. 2), shifted by controlled angle  $\varphi = 0 \div \pi$  rad. Let's take the  $u_{A1}$  pulses of the first (reference) section as the reference ones, relative to which the phase shift of the  $u_{A2}$  pulses of the second (controlled) section is carried out. The amplitudes of these pulses are equal to the supply voltage  $E$ , and their duty-cycle  $D$  is close to 0.5. To ensure zero voltage switching (ZVS) of transistors the operating frequency should be higher than the resonant frequency of the inverter, and a dead-time delay should be provided between the closed states of the transistor switches in each half-bridge [2, 13]. Multi-section converter may have several regulating sections, each of which may have its own phase shift [22].

**Presentation of the main material.** To simplify the analysis of the DCRC, we will assume that all its components are ideal, lossless, and the parameters of both resonant inverters are identical. Taking into account the filtering property of the resonant tank, we will analyze the inverter using the fundamental harmonic analysis (FHA) [2].

The equivalent circuit of the two-section inverter is shown in Fig. 3. The capacities of the coupling capacitors  $C_s$  are large enough, so they are absent in this scheme. According to the FHA method, the first harmonics of voltages  $u_{A1}$  and  $u_{A2}$  are represented by equivalent sources of sinusoidal voltages. The complex amplitudes of the sources of these voltages in the uncontrolled and in the controlled sections, respectively, are equal to:

$$\underline{E}_m = \frac{2E}{\pi}, \quad \underline{E}_N = E_m e^{-j\varphi}. \tag{1}$$

The equivalent resistance  $R_i$  of the inverter load (Fig. 3) is the input resistance of the rectifier with the load, reduced to the primary winding of the transformer. For a rectifier with the middle point of a transformer with ideal components, the resistance  $R_i$  is determined by the expression [25]:

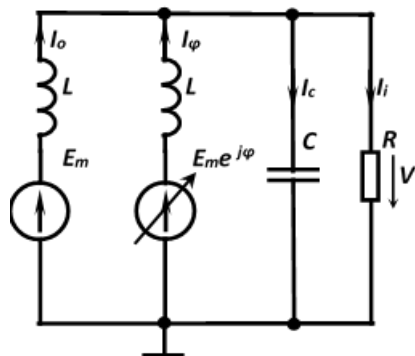


Figure 3. Converter equivalent circuit

$$R_i = \frac{\pi^2 n^2 R}{8}. \quad (2)$$

For the analysis, we will use the following notation and the relationship between the parameters.

Resonant frequency:

$$\omega_0 = \sqrt{\frac{2}{LC}}. \quad (3)$$

Characteristic impedance of resonant tank:

$$Z_0 = \frac{2}{\omega_0 C} \quad (4)$$

Quality factor of the resonant tank:

$$Q = \frac{2R_i}{Z_0}. \quad (5)$$

$\omega$  is the operating frequency;  $\Omega = \omega/\omega_0$  is the relative operating frequency.

The impedance of the parallel connection of resistance  $R_i$  and resonant capacitor  $C$  (Fig. 3) is equal to:

$$\underline{Z} = \frac{1}{j\omega C + \frac{1}{R_i}} = \frac{QZ_0}{2(1 + j\Omega Q)}. \quad (6)$$

The complex amplitude of the voltage across the resistance  $R_i$  is represented by the expression:

$$\underline{V}_i = \frac{\sum_{i=1}^2 \underline{E}_i g_i}{\sum_{i=1}^2 g_i + \frac{1}{\underline{Z}}} = \frac{1}{2} \frac{E_m \frac{1}{j\Omega Z_0} + E_m e^{j\varphi} \frac{1}{j\Omega Z_0}}{\frac{1}{j\Omega Z_0} + \frac{1 + j\Omega Q}{QZ_0}} = \frac{E}{\pi} \frac{1 + \cos \varphi - j \sin \varphi}{(1 - \Omega^2) + j \frac{\Omega}{Q}}. \quad (7)$$

The maximum value of the transfer function of the inverter according to the voltage of the first harmonic will occur at the phase shift  $\varphi=0$ :

$$M_{1\max} = \frac{|V_{i\max}|}{E_m} = \frac{1}{\sqrt{(1 - \Omega^2)^2 + \left(\frac{\Omega}{Q}\right)^2}}, \quad (8)$$

where  $|V_{i\max}|$  – module of the maximum value of (7).

At the same time, the quality factor, which provides the maximum voltage across the load of the inverter, is equal to:

$$Q = \frac{M_{1\max} \Omega}{\sqrt{1 - M_{1\max}^2 (1 - \Omega^2)^2}} \quad (9)$$

Complex current  $I_0$  of the uncontrolled section is equal to:

$$I_0 = \frac{E_m - V_i}{j\Omega Z_0} = \frac{2E}{\pi Z_0} \frac{\left[ -\Omega + \frac{1}{2\Omega} (1 - \cos \varphi) \right] + j \left[ \frac{1}{2\Omega} \sin \varphi + \frac{1}{Q} \right]}{j(1 - \Omega^2) - \frac{\Omega}{Q}} \quad (10)$$

Complex current  $I_\varphi$  of the controlled section is described by the expression:

$$I_\varphi = \frac{E_m e^{-j\varphi} - V_i}{j\Omega Z_0} = \frac{2E}{\pi Z_0} \frac{\left[ \left( \frac{1}{2\Omega} - \Omega \right) \cos \varphi + \frac{1}{Q} \sin \varphi - \frac{1}{2\Omega} \right] + j \left[ \left( \Omega - \frac{1}{2\Omega} \right) \sin \varphi + \frac{1}{Q} \cos \varphi \right]}{j(1 - \Omega^2) - \frac{\Omega}{Q}} \quad (11)$$

Complex current  $I_c$  of the resonant capacitor is given by the expression:

$$I_c = j \frac{2\Omega}{Z_0} U_i = \frac{2E}{\pi Z_0} \Omega \frac{\sin \varphi + j(1 + \cos \varphi)}{j(1 - \Omega^2) - \frac{\Omega}{Q}} \quad (12)$$

The current in the equivalent resistance  $R_i$  is equal to:

$$I_i = \frac{V_i}{R_i} = \frac{2E}{\pi Q Z_0} \frac{1 + \cos \varphi - j \sin \varphi}{j(1 - \Omega^2) - \frac{\Omega}{Q}} \quad (13)$$

Using expressions (10 ÷ 13) the dependences of normalized amplitudes of the currents  $I_c, I_0, I_\varphi, I_e$  (reduced to factor  $\frac{2E}{\pi Z_0}$ ) as a function of a phase shift are calculated and shown in Fig. 4. The inverter parameters are  $\Omega=1.08$  and  $Q=2.7$ .

The inverter power is determined by the following expression:

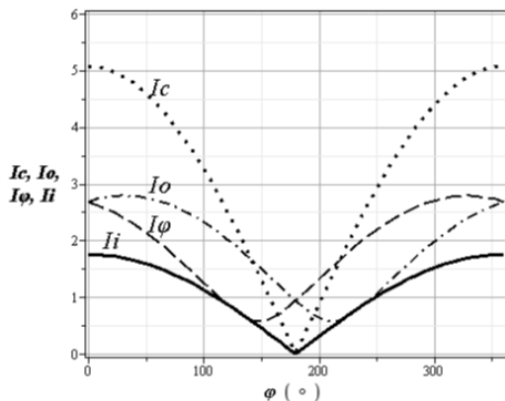


**Figure 4.** Dependencies of inverter current modules on the phase shift

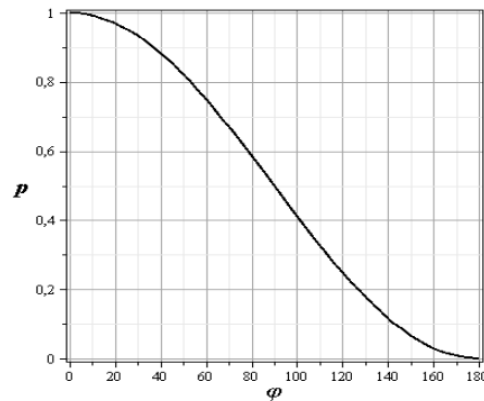


**Figure 5.** Dependencies of inverter normalized power on the phase shift

$$P = \frac{V_i I_i^*}{2} = \frac{2E^2}{\pi^2 Q Z_0} \frac{1 + \cos \varphi}{(1 - \Omega^2)^2 + \left(\frac{\Omega}{Q}\right)^2}. \quad (14)$$

Maximum power of the inverter (at  $\varphi=0$ ) is as follows:

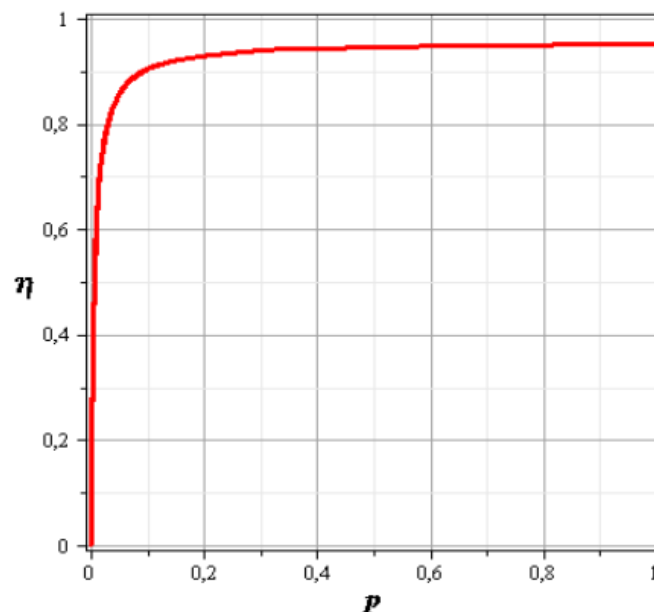
$$P_{\max} = \frac{2E^2}{\pi^2 Q Z_0} \frac{2}{(1 - \Omega^2)^2 + \left(\frac{\Omega}{Q}\right)^2}. \quad (15)$$

Figure 5 shows the dependence of relative power  $p = \frac{P}{P_{\max}}$  of inverter versus phase shift. The power is adjustable from 100% to 0 when changing the phase shift from 0 to 180°.

The efficiency of the inverter without taking into account the rectifier and transformer, is determined by the expression:

$$\eta_i = \frac{1}{1 + \frac{r_o I_o^2 + r_\varphi I_\varphi^2 + r_c I_c^2}{I_i^2 R_i}}, \quad (16)$$

where  $r_o$ ,  $r_\varphi$ ,  $r_c$  – correspondingly equivalent loss resistances of uncontrolled and controlled sections and capacitor  $C$ .



**Figure 6.** Dependencies of inverter efficiency on the normalized power

Fig. 6 shows the dependence of the efficiency on the relative power calculated for the same parameters  $\Omega=1.08$ ,  $Q=2.7$ , and the equivalent loss resistances are

$r_0 = r_\varphi = 2,5 \Omega$ ,  $r_c = 0,05 \Omega$ . As can be seen from this figure, when the relative power is reduced from 100% to about 10%, the efficiency decreases slightly and only at powers lower than 10% it drops sharply. Thus, the inverter provides effective regulation in a wide power range.

One of the conditions for the ZVS of transistors is to ensure a positive phase shift between the voltage and current of the transistor. Let's find the expressions for these phase shifts through the real and imaginary parts of the expressions for the complex powers of each of the sections. The complex power of the uncontrolled section is equal to:

$$\underline{S}_0 = \frac{1}{2} E_m I_0^* = \frac{E^2}{\pi^2 \Omega Z_0} \frac{\sin \varphi + 2 \frac{\Omega}{Q} + j(1 - \cos \varphi - 2\Omega^2)}{(1 - \Omega^2 \pi) - j \frac{\Omega}{Q}}. \tag{17}$$

The phase shift between voltage and current in an uncontrolled section can be determined through the arctangent of the ratio of the imaginary part of expression (17) to its real part, namely:

$$\varphi_0 = \arctg \frac{(1 - \Omega^2)(1 - \cos \varphi - 2\Omega^2) + \frac{\Omega}{Q} \left( \sin \varphi + 2 \frac{\Omega}{Q} \right)}{(1 - \Omega^2) \left( \sin \varphi + 2 \frac{\Omega}{Q} \right) - \frac{\Omega}{Q} (1 - \cos \varphi - 2\Omega^2)}. \tag{18}$$

The complex power of the controlled section is equal to:

$$\underline{S}_\varphi = \frac{1}{2} E_m e^{j\varphi} I_\varphi^* = \frac{E^2}{\pi^2 \Omega Z_0} \frac{(1 - \Omega^2) \left( \sin \varphi - 2 \frac{\Omega}{Q} \right) - j \frac{\Omega}{Q} (1 - \cos \varphi - 2\Omega^2)}{(1 - \Omega^2) - j \frac{\Omega}{Q}}. \tag{19}$$

The phase shift  $\varphi_\varphi$  between voltage and current in the controlled section is equal to:

$$\varphi_\varphi = \arctg \frac{(1 - \Omega^2)(1 - \cos \varphi - 2\Omega^2) + \frac{\Omega}{Q} \left( 2 \frac{\Omega}{Q} - \sin \varphi \right)}{-\frac{\Omega}{Q} (1 - \cos \varphi - 2\Omega^2) + (1 - \Omega^2) 2 \frac{\Omega}{Q} - \sin \varphi}. \tag{20}$$

According to expressions (14), (16), the dependences of the phase shift  $\varphi_0$  and phase shift  $\varphi_\varphi$  between voltages and currents on the phase shift  $\varphi$  for different values of the  $Q$  factor, respectively, in the uncontrolled (Fig. 7) and in the controlled (Fig. 8) sections are constructed. These dependences agree well with the results obtained in [24]. As a result of the computational experiment, it was established that at frequency values  $\Omega < 1.08$  the phase shift  $\varphi_\varphi$  in the control section becomes negative, and therefore, ZVS is lost. Therefore, in the two-section converter, the switching frequency should not be greater than this value.

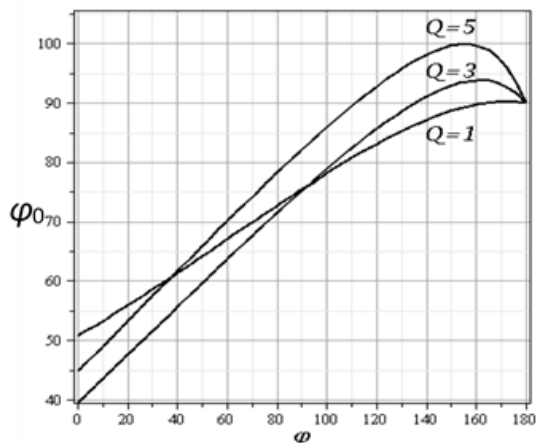


**Figure 7.** Dependencies of phase shift  $\varphi_0$  between voltage and current in uncontrolled section on the phase shift  $\varphi$  between sections for quality factors  $Q=1, Q=3, Q=5$

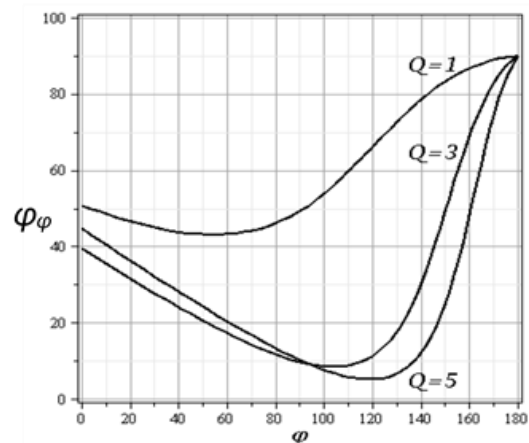


**Figure 8.** Dependencies of phase shift  $\varphi\varphi$  between voltage and current in controlled section on the phase shift  $\varphi$  between sections for quality factors  $Q=1, Q=3, Q=5$

The second condition of ZVS is the provision of a time delay between the closed states of the transistors, sufficient for the charge-discharge of their parasitic capacitances [13, 14].

**Verification of analysis results.** Based on the results of the analysis, a procedure was developed for calculating the parameters of the converter, which satisfies the specified values of supply voltage  $E$ , power  $P$  and voltage  $V_o$  in the load. The calculation procedure is described for converter with the following data  $P=60$  W,  $E=110$  V,  $V_o=26$  V, namely: 1) Load resistance  $R = V_o^2 / P = 11.3 \Omega$ ; 2) let us assume that transformer turn ratio is  $n=4$ ; 3) by expression (2), we determine the equivalent load resistance of the inverter  $R_i=223 \Omega$ ; 4) the amplitude of the voltage across the resistor  $R_i$ :  $V_{im} = \sqrt{2PR_i} = 167$  V; 5) the maximum value of the transfer function  $M_{1max} = V_{im} / E_m = 2.39$ ; 6) take  $\Omega = 1.08$ ; 7) from expression (9) we find  $Q=2.81$ ; 9) assuming the resonance frequency  $f_0=100$  kHz the inductance is determined  $L = 2R_i / (2\pi f_0 Q)^2 = 265 \mu\text{H}$ ; 10) the capacity is determined  $C = 2 / (\omega_0^2 L) = 19.1$  nF.

Using the PSIM 9.0 program, the simulation of DCRC with the parameters calculated above was carried out.

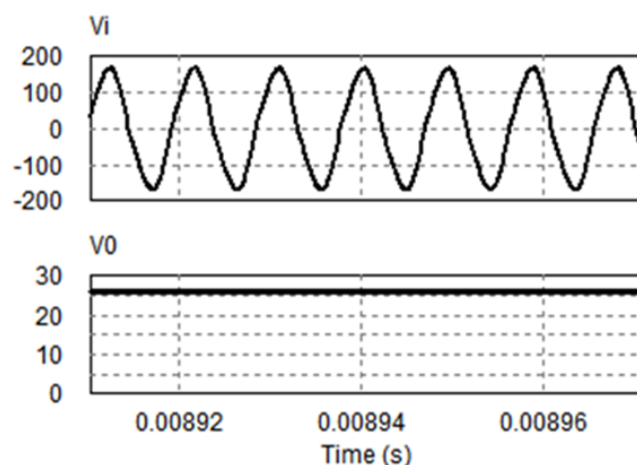


**Figure 9.** Simulation results: upper trace – resonant capacitor voltage; down trace – load voltage



**Table 1**

Results of calculation and simulation of output voltage for various phase shifts

$\varphi$ , (°)	Output voltage $V_0$ , V	
	Calculation	Simulation
0	25.98	26.31
30	25.10	25.36
60	22.50	22.78
90	18.37	18.65
120	12.99	13.23
150	6.72	6.86
180	0	0.09

The results of simulation for shift  $\varphi=0$  are presented in fig. 9, namely: the upper oscillogram is the voltage across the resonant capacitor (amplitude  $V_i=169$  V); the lower oscillogram is the output voltage ( $V_0=26.31$  V). Table 1 shows the results of calculation and simulation at different values of the shift  $\varphi$ . Thus, the obtained simulation results are in good agreement with the results of the analysis.

The conducted analysis can be extended to multi-section resonant inverters with phase power control. The issue of rational selection of the operating frequency at which the ZVS of transistors is guaranteed in the entire power range of the converter, as well as the study of ways to increase the efficiency of the converter, require further research.

**Conclusions.** A steady-state frequency-domain analysis of two-section resonant DC-to-DC converter with phase power control have been given. The maximum power of converter occurs during in-phase operation of the inverter sections. The inverter provides a wide range of power regulation in the load from maximum to zero when changing the phase shift between sections from 0 to 180°. The efficiency of the converter slightly decreases in the range of powers from 100% to 10% and only at powers less than 10% it drops sharply. At the same time, a change in the phase shift between the sections causes a change in the phase shift between the voltages and currents in its sections, which can put the inverter into capacitive mode of operation. Therefore, to ensure zero voltage switching of transistors it is necessary to select the operating frequency of the inverter by conducting a computational experiment at which the phase shifts between voltages and currents are guaranteed to be greater than zero. The conducted analysis can be extended to multi-section resonant inverters with continuous phase power control.

#### References

1. Vorperian V. and Cuk S. "A complete DC analysis of the series resonant converter," 1982 IEEE Power Electronics Specialists conference, Cambridge, MA, USA, 1982, p. 85–100. <https://doi.org/10.1109/PESC.1982.7072398>
2. Steigerwald R. I. A comparison of half-bridge resonant converter topologies. IEEE Transactions on Power Electronics. Vol. 3. P. 174–182. Apr. 1988. <https://doi.org/10.1109/63.4347>
3. Chen Y., Liu Y. F. Latest advances of LLC converters in high current, fast dynamic response, and wide voltage range applications. CPSS Transactions on Power Electronics and Applications. Volume 2. Issue 1. 2017. P. 59–67. <https://doi.org/10.24295/CPSSTPEA.2017.00007>

4. Musavi F., Craciun M., Gautam S., Eberle W., Dunford W. "A Novel Multi-resonant DC-DC Converter with Wide Output-Voltage Range Battery Charging Applications" IEEE Transactions on Power Electronics. Vol. 28. No. 12. P. 5437–5445. 2013. <https://doi.org/10.1109/TPEL.2013.2241792>
5. Brañas C., Viera J. C., Azcondo F. J., Casanueva R., Anseán D. "Multiphase resonant converter with output current multiplier for battery charger applications" Proceedings of the 42nd Annual Conference of the Industrial Electronics Society (IECON), Florence, 2016, 5639–5644. <https://doi.org/10.1109/IECON.2016.7794146>
6. Pinuela M., Yates D.C., S. Lucyszyn, P. Mitcheson. "Maximizing DC-to-Load Efficiency for Inductive Power Transfer" IEEE Transactions on Power Electronics. Vol. 28. No. 5. P. 2437–2447. May 2013. <https://doi.org/10.1109/TPEL.2012.2215887>
7. Wang T. W., Lin T. T. "Wireless Power Transmission on Biomedical Applications". In book: Microwave Technologies, Publisher: IntechOpen. March 2022. P. 18. <https://doi.org/10.5772/intechopen.103029>
8. Wang H., Zanchetta P., Clare J., Ji C. "Modelling and control of a zero current switching high-voltage resonant converter power supply for radio frequency sources" IEEE Transactions on Power Electronics. Vol. 5. No. 4. P. 401–409. 2012. <https://doi.org/10.1049/iet-pel.2010.0400>
9. Ji C., Zanchetta P., Carastro F., Clare J. C. "Repetitive Control for High-Performance Resonant Pulsed Power Supply in Radio Frequency Applications". IEEE Transactions on Industry Applications. Vol. 50. No. 4. 2014. P. 2660–2670. <https://doi.org/10.1109/TIA.2013.2292997>
10. Shrivastava A., Singh B. LLC Series Resonant Converter Based LED Lamp Driver with ZVS / 2012 IEEE Fifth Power India Conference, Official. URL: <http://ieeexplore.ieee.org/document/6479553/>. <https://doi.org/10.1109/PowerI.2012.6479553>
11. Jagadeesh R., Vishwanathan N., Porpandiselvi S. An Efficient Parallel Resonant Converter for LED Lighting / Proceedings of the National Power Systems Conference (NPSC) – 2018, India 5 p. <https://doi.org/10.1109/NPSC.2018.8771439>
12. Dobi A. H. M., Sahid M. R., Sutikno T. Overview of Soft-Switching DC-DC Converters. International Journal of Power Electronics and Drive System (IJPEDS). Vol. 9. No. 4. December 2018. P. 2006–2018. <https://doi.org/10.11591/ijpeds.v9.i4.pp2006-2018>
13. Ashique R., Salam Z., Maruf M., Shihavuddin A., Islam M.I., Rahman M., Kotsampopoulos P., Fayek H. A Comparative Analysis of Soft Switching Techniques in Reducing the Energy Loss and Improving the Soft Switching Range in Power Converters. March 2022. Electronics. 11 (7) 20. P. 1062. <https://doi.org/10.3390/electronics11071062>
14. Vorperian V. and Cuk S. "A Complete DC Analysis of the Series Resonant Converter," Proc. IEEE PESC'82, 1982. <https://doi.org/10.1109/PESC.1982.7072398>
15. Yang J. T. and Lee F. C. "Computer Aided Design and Analysis of Series Resonant Converters," Proc. IEEE IAS '87, 1987.
16. Liu R., Batarseh I., Lee C. Q. "Comparison of Capacitively and Inductively Coupled Parallel Resonant Converters," IEEE Trans. on Power Electronics. 1993. P. 445–454. Vol. 8. Issue 4. <https://doi.org/10.1109/63.261015>
17. Kang Y. G., Upadhyay A. K., Stephens D. "Analysis and Design of a Half Bridge Parallel Resonant Converter Operating Above Resonance," Proc. IEEE IAS '98, 1998, p. 827–836.
18. Zaki M., Bonsall A., Batarseh I., "Performance Characteristics for the Series Parallel Resonant Converter," Proc. Southcon '94, 1994, p. 573–577. <https://doi.org/10.1109/SOUTHCON.1994.498168>
19. Bhat A. K. S., "Analysis, Optimization and Design of a Series Parallel Resonant Converter," Proc. IEEE APEC '90, 1990, p. 155–164. <https://doi.org/10.1109/APEC.1990.66407>
20. Salem M., Jusoh A., Idris N. R. N., Sutikno T., Buswig Y. M. Y. "Phase-shifted Series Resonant Converter with Zero Voltage Switching Turn-on and Variable Frequency Control". International Journal of Power Electronics and Drive Systems. Vol. 8. No. 3. 2017. P. 1184–1192. Doi: 10.1159/ijpeds.v8s3.pp1184-1192. <https://doi.org/10.1159/ijpeds.v8.i3.pp1184-1192>
21. Branas C., Azcondo F.J., Casanueva R. "A generalized study of multiphase parallel resonant inverters for high-power applications", IEEE Transactions on Circuits and Systems I. 2008. Vol. 55. No. 7. P. 2128–2138. <https://doi.org/10.1109/TCSI.2008.916704>
22. Lupenko A. Step-continuous phase power control of multi-section resonant inverter. Computational problems of electrical engineering. Vol. 10. No. 2. 2020. P. 7–12.
23. Kazimierczuk M. K. Phase-controlled series-parallel resonant converter. IEEE Transactions on Power Electronics. Vol. 8. No. 3. 1993. P. 309–319. <https://doi.org/10.1109/63.233288>
24. Kazimierczuk M. K., Czarkowski D. Resonant power converters, 2nd Edition. John Wiley & Sons. 2011. 632 p.
25. Gilbert A. J., Bingham C. M., Stone D. A., Foster M. P. Normalized Analysis and Design of LCC Resonant Converters. IEEE Transactions on Power Electronics December 2007. 22 (6): 2386–240. <https://doi.org/10.1109/TPEL.2007.909243>.

УДК 621.314

**АНАЛІЗ ДВОСЕКЦІЙНОГО РЕЗОНАНСНОГО ПЕРЕТВОРЮВАЧА НАПРУГИ З ФАЗОВИМ РЕГУЛЮВАННЯМ ПОТУЖНОСТІ****Анатолій Лупенко; Леонід Мовчан; Іван Сисак***Тернопільський національний технічний університет імені Івана Пулюя,  
Тернопіль, Україна*

**Резюме.** Робота присвячена аналізу високоефективного двосекційного резонансного перетворювача постійної напруги з фазовим регулюванням потужності в широкому діапазоні при його роботі на сталій частоті. Кожна із інверторних секцій перетворювача виконана за схемою паралельного резонансного напівмостового інвертора напруги зі спільним їх резонансним конденсатором, який через трансформатор, випрямляч із середньою точкою і згладжувальний фільтр під'єднано до навантаження. Інверторну частину перетворювача розглянуто як граничний випадок багатосекційного резонансного інвертора, в якому одна із секцій є опорною, відносно вихідних імпульсів якої здійснюється регулювання фазового зсуву вихідних імпульсів іншої секції. Частота комутації перетворювача є постійною, що покращує його електромагнітну сумісність у порівнянні з перетворювачами з частотним регулюванням. Аналіз виконано методом основної гармоніки. Встановлено аналітичні вирази для комплексних напруг та струмів у обох секціях перетворювача. Отримано регульовальну характеристику – залежність потужності перетворювача від фазового зсуву між імпульсами напівмостових інверторних секцій. Розглянуто питання роботи транзисторних ключів секцій у режимі їх комутації з нульовою напругою. Фазовий зсув між секціями при регулюванні потужності впливає на фазовий зсув між напругами і струмами у його секціях, що може перевести інвертор в смісний режим роботи. Тому при проектуванні перетворювача для забезпечення комутації ключів при нульовій напрузі необхідно шляхом проведення обчислювального експерименту вибрати робочу частоту інвертора такою, за якої фазові зсуви між напругами і струмами є гарантовано більшими від нуля. Проаналізовано залежність ККД перетворювача від потужності. Показано, що ККД незначно зменшується при зменшенні потужності в широкому діапазоні потужностей і лише на потужностях менших за 10% від максимальної, різко падає. Проведено верифікацію запропонованого аналізу шляхом імітаційного моделювання схеми перетворювача за допомогою PSIM-програми моделювання пристроїв силової електроніки. Результати моделювання добре узгоджуються з результатами аналізу.

**Ключові слова:** двосекційний резонансний перетворювач, комутація при нульовій напрузі, потужність, фазове регулювання, ККД.

[https://doi.org/10.33108/visnyk\\_tntu2023.02.087](https://doi.org/10.33108/visnyk_tntu2023.02.087)

Отримано 02.03.2023